

## Individual variation in contractile cost and recovery in a human skeletal muscle

MICHAEL L. BLEI\*†, KEVIN E. CONLEY‡§, IB R. ODDERSON\*, PETER C. ESSELMAN\*,  
AND MARTIN J. KUSHMERICK‡¶

Departments of \*Rehabilitation Medicine, †Radiology, and ‡Physiology and Biophysics, University of Washington Medical Center, Seattle, WA 98195

Communicated by C. Richard Taylor, April 30, 1993 (received for review March 5, 1993)

**ABSTRACT** This study determined the variation among individuals in ATP use during contraction and ATP synthesis after stimulation in a human limb muscle. Muscle energetics were evaluated using a metabolic stress test that separates ATP utilization from synthesis by  $^{31}\text{P}$  NMR spectroscopy. Epicutaneous supramaximal twitch stimulation (1 Hz) of the median and ulnar nerves was applied in combination with ischemia of the finger and wrist flexors in eight normal subjects. The linear creatine phosphate (PCr) breakdown during ischemic stimulation defined ATP use ( $\Delta\text{PCr}$  per twitch or  $\sim\text{P}/\text{twitch}$ ) and was highly reproducible as shown by the relative standard deviation [(standard deviation/mean)  $\times$  100] of 11% in three repeated measures. The time constant of the monoexponential PCr change during aerobic recovery represented ATP synthesis rate and also showed a low relative standard deviation (9%). Individuals were found to differ significantly in both mean  $\sim\text{P}/\text{twitch}$  (PCr breakdown rates, 0.29–0.45% PCr per sec or % PCr per twitch; ANOVA,  $P < 0.001$ ) and in mean recovery time constants (41–74 sec; ANOVA,  $P < 0.001$ ). This range of  $\sim\text{P}/\text{twitch}$  corresponded with the range of fiber types reported for a flexor muscle. In addition,  $\sim\text{P}/\text{twitch}$  was negatively correlated with a metabolite marker of slow-twitch fiber composition ( $\text{P}_i/\text{ATP}$ ). The nearly 2-fold range of recovery time constants agreed with the range of mitochondrial volume densities found in human muscle biopsies. These results indicate that both components involved in the muscle energy balance—oxidative capacity and contractile costs—vary among individuals in human muscle and can be measured noninvasively by  $^{31}\text{P}$  NMR.

Muscle has the ability to perform a wide range of functions that depend on the metabolic and contractile properties of the underlying fibers and the recruitment pattern of the motor units. Most muscles contain a mixture of fiber types displaying a continuum of contractile speeds and metabolic capacities ranging from the slow-twitch oxidative type I fibers to the fast-twitch glycolytic type II fibers (1). Animal studies have shown that fibers differ in the contractile cost per twitch (2, 3). In addition, the rate of ATP resynthesis also varies among fibers depending on the oxidative phosphorylation capacity. The lower cost per twitch and higher oxidative capacity of slow-twitch fibers allow higher sustained twitch rates than fast-twitch fibers (3, 4). Thus, both contractile and metabolic properties are critical to sustained muscle performance.

Human muscle has also been found to have a range of fiber types based on studies of cadaveric muscle and fresh muscle biopsies. Recent  $^{31}\text{P}$  NMR studies have suggested that metabolic differences exist among fibers within human muscle (5, 6) and between muscles of individuals at distinct training levels (7, 8). However, it is not clear whether the fibers also differ in contractile costs in humans. In animal studies,

fast-twitch muscle has a higher contractile cost, while differences in the metabolic capacity are seen as a slower recovery rate after stimulation compared to more oxidative muscles (3). Such a quantitative assessment of both components of the energy balance has not been made for humans to determine whether cost per twitch and oxidative capacity differ among muscles.

Assessment of these muscle energetic properties requires evaluating both the rate of energy utilization (ATPase rate or cost per twitch) and the rate of energy synthesis (oxidative phosphorylation rate). We have reported (9) on a  $^{31}\text{P}$  NMR spectroscopic procedure that separates the chemical changes during contractile activity from those during recovery in human limb muscle, which is termed the *quantitative energetic stress test* (QUEST). The dynamic changes in creatine phosphate (PCr) content during an external stimulation and recovery protocol provide an assessment of the components of energy balance in exercising muscle.

The purpose of this study is to determine whether reproducible differences in these functional bioenergetic properties exist in the forearm musculature among humans. To achieve this goal, we assess (i) the reproducibility and sensitivity of the PCr breakdown rate (ATPase rate) and the recovery rate (ATP synthesis rate) in normal subjects and (ii) the natural variation of these contractile and metabolic properties among individuals.

### METHODS

**Subjects.** Eight subjects (four male and four female) were drawn from a population of normal volunteers (25–60 years old) who were active but were not engaged in a specific training program. Voluntary consent was obtained from each subject prior to participation under an experimental protocol approved by the Human Subjects Office of the University of Washington.

**Experimental Design.** The QUEST protocol was used in this experiment as described (9). To test the accuracy and reproducibility of this protocol, the procedure was repeated on the same day and 1 week or more later. Briefly, this protocol separates ATP utilization from its resynthesis by using the magnitude and time course of changes in PCr. Spectral data were obtained at 9-sec intervals for a total duration of 23 min.

**$^{31}\text{P}$  NMR Acquisition and Spectral Analysis.** The experiments used a 2.0-tesla General Electric CSI spectrometer with a one-pulse  $^{31}\text{P}$  NMR acquisition. An inductively coupled 4.5-cm diameter circular surface coil was centered over

Abbreviations: PCr, creatine phosphate; QUEST, quantitative energetic stress test.

†Present address: Department of Rehabilitation Medicine, University of Colorado Health Sciences Center, 4200 East 9th Avenue, Campus Box C243, Denver, CO 80262.

§To whom reprint requests should be addressed at: NMR Research Laboratory, Department of Radiology, SB-05, University of Washington Medical Center, Seattle, WA 98195.

The publication costs of this article were defrayed in part by page charge payment. This article must therefore be hereby marked "advertisement" in accordance with 18 U.S.C. §1734 solely to indicate this fact.

the flexor digitorum superficialis of the arm. A high-resolution resting control spectrum was obtained under fully relaxed conditions for each subject, using a 20-sec interpulse delay for 16 acquisitions with a  $\pm 2000$ -Hz spectral width and 2000 data points. The free-induction decays were processed with baseline correction, Fourier-transformed into spectra, and analyzed by the PIQABLE algorithm to estimate the baseline along with the peak positions and areas (10, 11). Peak areas were fitted to Lorentzian and Gaussian line shapes using a least-squares nonlinear curve-fitting routine in the frequency domain (12).

In the ischemic stimulation and recovery experiment, 155 sequential spectra were obtained under partly saturated NMR conditions. One dummy scan was followed by four acquisitions, each with a 1.76-sec interpulse delay (9 sec per spectrum). The resultant spectra typically had a 20:1 signal-to-noise ratio for PCr, as shown in Fig. 1. The free-induction decays were line-broadened with the line width of the unfiltered PCr peak and the resultant spectra were compared to a high signal-to-noise spectrum acquired under the same pulsing conditions using a least-squares comparison after correction for partial saturation using the fully relaxed spectrum (13).

**Muscle Stimulation.** Nerve stimulation of the median and the ulnar nerves activated the finger and wrist flexors over a region larger than the volume subtended by the surface coil (9). Full activation was established as the minimal voltage needed to elicit full excitation of the muscle as measured by the compound muscle action potential recorded on the skin surface.

**Statistics.** For each individual, the rate of PCr utilization was estimated by the slope of a linear regression of PCr area vs. time. PCr recovery time constants were estimated from a monoexponential fit using nonlinear regression for each experiment. Means were distinguished among subjects using an ANOVA and Fisher multiple *t* test. The null hypothesis was rejected at the 0.05 level of probability.

## RESULTS

**<sup>31</sup>P NMR Spectra in Resting Aerobic Muscle.** A fully relaxed spectrum was taken at the beginning of each experiment to

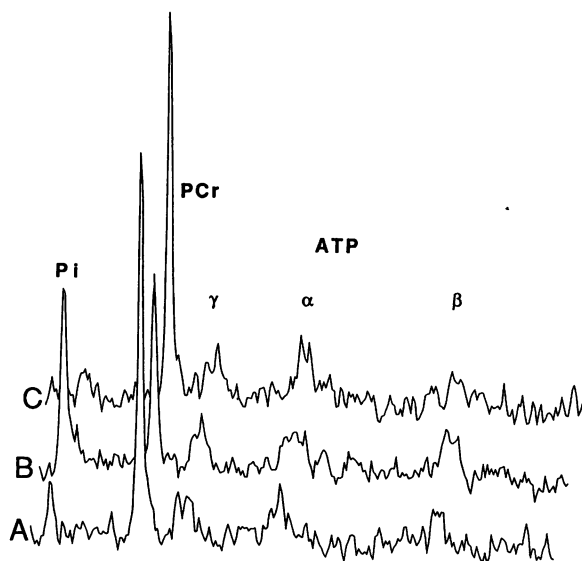


FIG. 1. Stack plot of the partially saturated spectra under the experimental conditions used to follow the high-energy phosphate dynamics through the protocol (four acquisitions, 9 sec total; apodized with a line broadening of 4 Hz). Spectra: A, control condition in resting muscle; B, poststimulation ischemia; C, recovery.

quantify the ratios of high-energy phosphate peak areas. Fig. 1 displays a stack plot of the spectra taken in the resting muscle, during poststimulation ischemia, and after recovery under the pulsing and acquisition conditions used in the experimental protocol. These spectra are representative of those used for determining the dynamics of PCr breakdown and recovery shown in the full experimental protocol in Fig. 2.

**QUEST Protocol.** The PCr,  $P_i$ , and ATP dynamics during the ischemic stimulation and recovery protocol resulted in a similar decrease in the PCr/ATP ratio for the subjects from  $3.96 \pm 0.34$  (mean  $\pm$  SD) at rest to  $2.31 \pm 0.65$  during stimulation. There was no difference in the PCr/ATP ratio attained during stimulation among the subjects (ANOVA,  $P = 0.32$ ). The change in the fraction of PCr per total phosphate from rest through stimulation ( $-0.32 \pm 0.057$ ) was stoichiometric with the increase fraction of  $P_i$  ( $+0.31 \pm 0.053$ ). Since no change in ATP was found, the high-energy phosphate dynamics during our protocol were restricted to the stoichiometric changes in PCr and  $P_i$ . This stoichiometry allowed us to correct for signal loss or movement artefacts during the procedure by expressing high-energy phosphate changes as PCr/(PCr +  $P_i$ ). All results were expressed normalized to the control values (i.e., PCr/(PCr +  $P_i$ , normalized to unity). The percent breakdown (i.e., % PCr per sec or % PCr per twitch) was used to express the depletion rate. To determine whether this normalization affected the time course of the PCr recovery, we examined experiments where no motion artefacts were apparent and found that the time constant of recovery ( $\tau$ ) did not significantly differ whether PCr alone or PCr/(PCr +  $P_i$ ) was used in the calculation ( $P > 0.2$ ,  $n = 11$ ; paired *t* test). We used these changes in PCr to separate ATP utilization (PCr breakdown) from its resynthesis (PCr recovery) as illustrated in Fig. 2.

**PCr Utilization Rates.** With stimulation, the PCr content decreased rapidly until near the end of the 128-sec stimulation period when deviations from a linear rate of decline were clearly seen. The data for PCr depletion were fitted well by a linear function through the first 108 sec of stimulation. The slope of this depletion provided a measure of the rate of PCr breakdown. During the final seconds of the stimulation period, a small deviation from linearity consistently occurred and these three points were not included in the calculated slope. The initial rates of PCr depletion were reproducible in

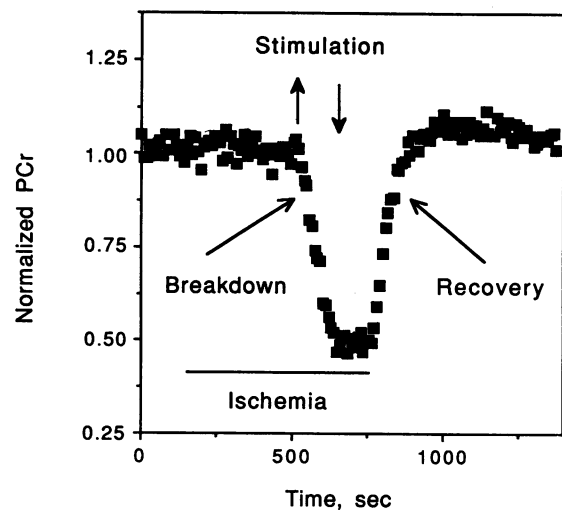


FIG. 2. PCr dynamics showing the ischemic period, stimulation duration, and time course of recovery in one individual. Normalized data were used to determine the PCr breakdown rate and time constant of PCr recovery. Each point represents four acquisitions taken over 9 sec.

the same individual, as shown by the relative standard deviation of the triplicate measures in each individual  $[(SD/\text{mean}) \times 100]$ , which averaged 11%. The reliability of this procedure was further evaluated by calculating the correlation coefficient ( $r$ ) of the linear regression of the eight individual rates between experiments ( $r = 1.0$  for exact reliability). This test/retest reliability for repeated experiments was 0.7 for the same day and 0.8 for 1 week later. We have previously shown that there is little ATP synthesis detectable during the stimulation period; therefore, the observed rate of PCr depletion is equal to the rate of ATP utilization (9). This breakdown rate also measures the ATP cost per twitch since the twitch frequency was constant.

The mean of the three determinations of the PCr breakdown rate ( $\sim P/\text{twitch}$ ) for each subject significantly differed among individuals (ANOVA;  $P < 0.001$ ) and ranged from 0.29 to 0.45% PCr per sec or per twitch in our subjects. Fig. 3 shows a single experiment for two individuals that represents the range of breakdown rates among the subjects. A comparison of the mean rates in Fig. 4 shows the range of values and identifies the differences among the subjects based on a multiple  $t$  test (Fig. 4). For example, the largest means—subjects F and K—were different from the means of subjects M, N, S, I, and R. This difference is designated by letters F and K adjacent to the underscoring spanning bars M, N, S, I, and R in Fig. 4. Similarly, subject P was significantly different from the underscored subjects: bars M and N. Thus these results indicate that PCr breakdown rate was highly reproducible in the individuals studied and was sensitive enough to distinguish individual differences among these normal subjects. The first major result of these experiments is that  $\sim P/\text{twitch}$  differed 1.6-fold among our subjects.

**Correlation of ATP Utilization Rate with Resting Metabolite Composition.** One hypothesis to explain the range in  $\sim P/\text{twitch}$  among our subjects is that each individual's forearm musculature differs in its composition of fiber types. In animal muscles there are clear differences in the content of high-energy phosphates and other metabolites in individual muscles composed of different fiber types (14). The largest quantitative difference in the animal muscles was in the  $P_i$  content, which was significantly higher in muscles with a high fractional composition of slow-twitch oxidative (type I) fibers (14). To test whether a similar correlation existed in our subjects, we compared the PCr breakdown rates to resting high-energy phosphate levels. We postulated that phosphorylated metabolite levels at rest are cellular markers indicative of fiber type distribution and, therefore, of the ATPase rates, such as myosin ATPase, in the fiber. Fig. 5A shows the significant correlation between PCr breakdown rate and the resting  $P_i/\text{ATP}$  level in our subjects ( $P < 0.02$ ). In contrast,

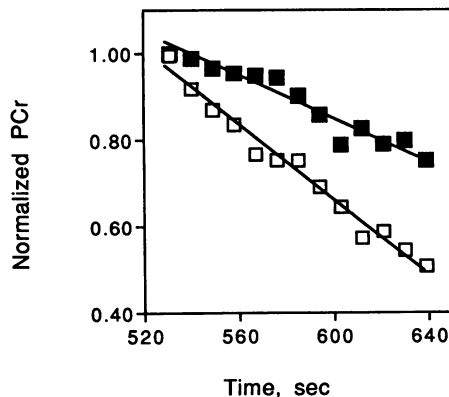


FIG. 3. PCr breakdown for two individuals (■ and □) during the first 108 sec of stimulation illustrating the range found in the mean breakdown slopes among the experimental subjects.

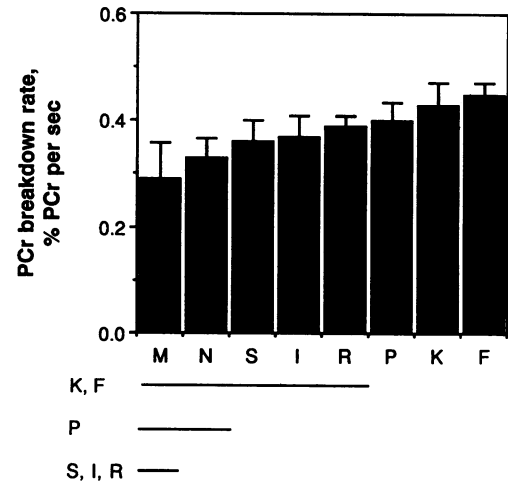


FIG. 4. Comparison of the PCr breakdown rate (mean  $\pm$  SD) among the subjects. The significant differences are shown by letters adjacent to the underscored bars. For example, the bars for subjects K and F are different from those of M, N, S, I, and R.

no correlation was found between PCr breakdown rate and PCr/ATP (Fig. 5B;  $P = 0.39$ ), which agrees with the small difference in PCr and PCr/ATP levels ( $<15\%$ ) found in human fiber types (15, 16). The negative slope in Fig. 5A indicates that PCr breakdown rate decreases as  $P_i/\text{ATP}$  ratio increases, as expected from mammalian muscle studies. Thus the PCr breakdown rates ( $\sim P/\text{twitch}$ ) among our subjects are correlated with a marker of fiber type found in mammalian muscle studies.

**Recovery Rate.** The oxidative component of the muscle energy balance was measured as the rate of PCr resynthesis once blood flow commenced after release of the ischemic cuff. Aerobic PCr recovery was monitored for 10 min after restoration of blood flow to the arm as shown in Fig. 2 for a single subject. No recovery was detectable in the first spectrum (9 sec) after release of the cuff, but PCr recovery followed an approximately exponential time course thereafter. The time constant ( $\tau$ ) of this recovery was determined from a monoexponential fit to these data.

We found that  $\tau$  of the PCr recovery in the three repetitions of the protocol was reproducible in each subject, with an average relative standard deviation of 9%. The reliability for repeat experiments of this procedure was 0.8 on the same day and 0.7 a week later. Thus the repeatability and reliability of the measures of the ATP cost per twitch and the recovery ATP synthesis rate were similar. However, there was no significant correlation between the ATPase rate ( $\sim P/\text{twitch}$ ) and ATP synthesis rate (or  $\tau$ ) in our subjects.

The mean values of  $\tau$  for the three runs ranged from 41 to 74 sec and significantly differed among the subjects (ANOVA;  $P < 0.001$ ). Fig. 6 shows a single experiment for two individuals that represent the range of recovery time courses among the subjects. Time constants calculated for these two recoveries are illustrated in the figure insert. Fig. 7 shows the results for each subject with the differences among the individuals as a multiple comparison of means (Fig. 7). The underscored values in this comparison significantly differ from the value denoted by the adjacent letter. Thus, the second major result of these experiments is that the PCr recovery time course differed among the subjects by 1.8-fold.

## DISCUSSION

The energy balance in muscle during exercise depends on matching the contractile demand for energy (ATP use) with

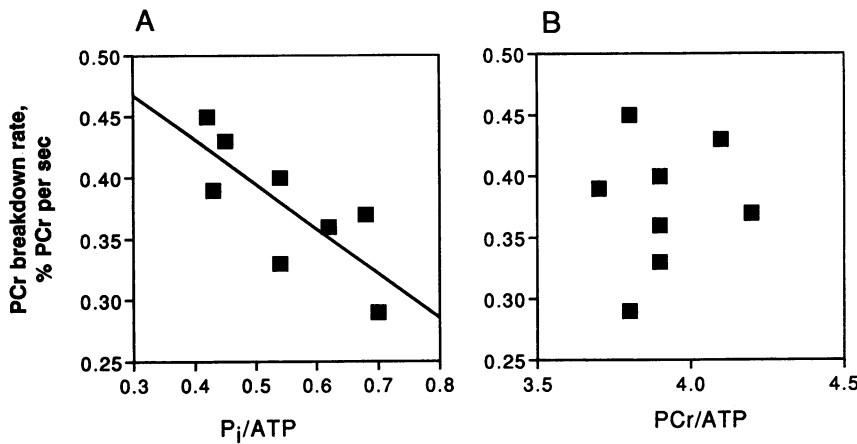


FIG. 5. PCr breakdown rate as a function of resting metabolite levels in the eight experimental subjects. (A) Correlation of mean breakdown rate vs. mean resting  $P_i/ATP$  level ( $y = -0.36x + 0.58$ ;  $r = 0.78$ ;  $P < 0.02$ ). (B) Plot of mean breakdown rate vs. mean resting  $PCr/ATP$  level.

metabolic energy supply (ATP synthesis). Differences in sustainable human muscle performance have been attributed solely to the oxidative capacity of the muscle (7, 8). Our goal was to test quantitatively in intact human muscle for variation in contractile cost as well. We assessed the individual variation in the capacity for ATP utilization and resynthesis to determine whether functional properties reflect the ranges in fiber types and metabolic properties.

**Separation of PCr Breakdown from Recovery.** The ischemic stimulation and recovery protocol achieves a separation of these contractile and metabolic processes using the dynamic changes in PCr content during stimulation and recovery (Figs. 1 and 2). By depleting the muscle of oxygen prior to stimulation, the PCr breakdown during activation measures the rate of ATP use by the muscle in the absence of simultaneous ATP synthesis by the mitochondria (9). Restoration of blood flow and the subsequent aerobic recovery provides a measure of the ATP synthesis rate. These features of the QUEST protocol are important in defining the contractile and metabolic properties of muscle. Fast-twitch fibers have high ATPase rates and large cost per twitch but generally have low mitochondrial contents, while the opposite is true for slow-twitch fibers. The differences in ATPase rate and mitochondrial content are measured as the  $\sim P/twitch$  and recovery rate after stimulation. These rates provide functional and

mechanistically interpretable measurements of the ATP supply and demand components of the muscle energy balance.

**PCr Breakdown Rate.** The first component of the muscle energy balance is the ATP cost of contraction. To determine the reproducibility and sensitivity of the procedure for measuring  $\sim P/twitch$ , we examined the initial rate of PCr depletion in eight subjects fitted by a linear function as shown in Fig. 3. These slopes were very reproducible; three repeat measures for each individual had a relative standard deviation of 11%. Since PCr levels differ little between human fiber types, the range of % PCr per twitch represents differences in the  $\sim P/twitch$  among our subjects and suggests underlying differences in the fiber type composition of these muscles. Kushmerick *et al.* (14) have established that slow-twitch fibers contain a higher  $P_i$  level than fast-twitch muscles in mammalian muscles of different species. Fig. 5A shows that the  $\sim P/twitch$  is negatively correlated with  $P_i/ATP$ . Thus, the muscles with the highest  $\sim P/twitch$  have the low  $P_i/ATP$  indicative of a faster-twitch fiber, whereas the lowest  $\sim P/twitch$  is found in individuals with the high  $P_i/ATP$  indicative of a slower-twitch muscle. In contrast,  $PCr/ATP$  varies little across fibers and no correlation was found between  $\sim P/twitch$  and the  $PCr/ATP$  ratio (Fig. 5B). This is consistent with the similar  $PCr/ATP$  ratios found in analyses of single fibers and whole muscles containing different compositions of fiber types in humans (15, 16). Thus, the individual differences in  $\sim P/twitch$  corresponded with differences in  $P_i$  content indicative of fiber type in mammalian muscles.

Surgical biopsies of one muscle sampled in our protocol, the flexor carpi radialis, reveal a range in fast-twitch (type II)

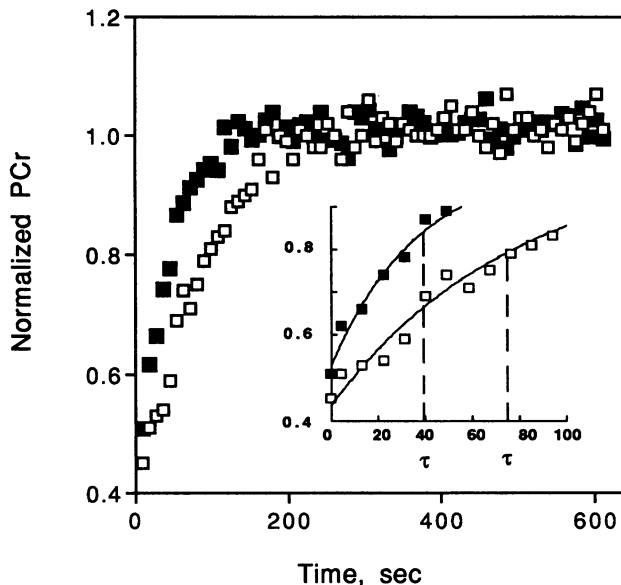


FIG. 6. Time course of PCr recovery in two individuals (■ and □) representing the range of rates in our subjects. (Inset) Range of individual recovery time courses. The time constant ( $\tau$ ) for each recovery is shown by the vertical dashed lines.

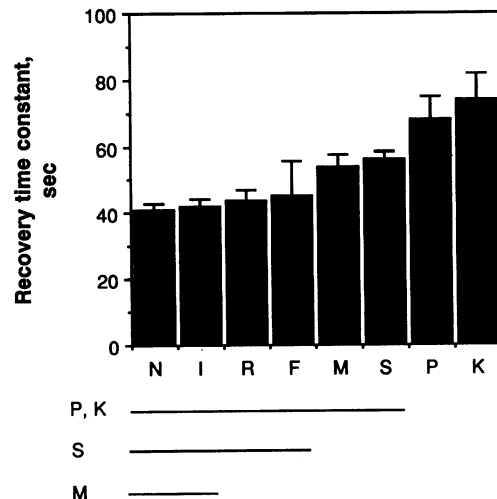


FIG. 7. Comparison of PCr recovery time constants ( $\tau$ , sec) among the experimental subjects as determined by multiple  $t$  test as described in Fig. 4.

content from 35 to 85% fast twitch fibers.<sup>||</sup> The myosin ATPase activity of a fiber, and therefore the  $\sim P$ /twitch, varies in direct proportion to maximal shortening velocity (1, 17). Thus the 5-fold range in maximum velocity between fast- and slow-twitch fibers should be reflected in as large as a 5-fold difference in ATPase rates among fiber types. Using this range of rates (fast, relative rate of 5; slow, relative rate of 1), we estimated the relative ATPase rates for two extreme muscle compositions reported for the flexor carpi radialis: 15% type I and 85% type II vs. 65% type I and 35% type II. A relative ATPase rate of 4.4 results from 15% type I ( $1 \times 0.15 = 0.15$ ) and 85% type II ( $5 \times 0.85 = 4.25$ ), while a relative rate of 2.4 results from a 65%/35% fiber composition ( $1 \times 0.65 = 0.65$  and  $5 \times 0.35 = 1.75$  thus  $0.65 + 1.75 = 2.4$ ). These ATPase activities result in a 4.4/2.4 or 1.8-fold range, which is similar to the  $\sim P$ /twitch range (1.6-fold) found for our ischemic stimulation protocol. In addition, the measured breakdown rates correspond to 0.09–0.15 mM ATP per twitch (9), which is close to the 0.08 mM ATP per twitch reported for the human vastus lateralis (18). Thus the individual variation in  $\sim P$ /twitch corresponded with the relative range of ATPase rates estimated from the published fiber type composition of the wrist flexor muscles as well as with a metabolite marker of myosin isoform content ( $P_i$ /ATP). These results indicate that  $\sim P$ /twitch is not fixed but varies in proportion to the myosin isoform content and fiber type composition of human muscle.

**PCr Recovery.** The second component of muscle energy balance is oxidative ATP synthesis. The synthesis rate was characterized by the time constant of PCr recovery after restoration of blood flow. Individual recovery time constants differed by 1.8-fold (Figs. 6 and 7) and were also very reproducible in three repeat measures (relative standard deviation = 9%). The rate of recovery as measured by the time constant should reflect the oxidative capacity of the muscle, since (i) the intracellular  $H^+$  and ATP levels are not significantly altered during the QUEST protocol and (ii) PCr/ATP did not differ among the subjects at rest or after stimulation. The similar PCr/ATP ratios mean that the signal for oxidative phosphorylation (e.g., ADP) did not differ among the subjects at the start of recovery (9). With each subject recovering from a similar PCr/ATP level, the time course of recovery (e.g.,  $\tau$ ) will reflect the oxidative capacity of the muscle, as Meyer (19) has shown. To our knowledge, the range of mitochondrial content or oxidative capacity of the finger and wrist flexor muscles is not available to compare against these time constants. However, biopsies of the vastus lateralis from normal subjects in the age range used in this study had mitochondrial volume densities ranging nearly 2-fold from 4 to 7% (20). This range is similar to the 1.8-fold range of time constants found among our subjects. Thus our results show that both contractile costs and oxidative synthesis rate differed among our subjects in accordance with the variation in fiber-type composition and mitochondrial content of human muscle.

Most NMR methods of evaluating muscle properties do not separate the components of muscle energy balance but instead use the splitting of the  $P_i$  peak (5, 6, 21) or the steady-state levels of  $P_i$ /PCr during exercise to estimate the functional properties of muscle (cf. 7, 8). However, neither the pH of the  $P_i$  peak nor the  $P_i$ /PCr level uniquely characterize muscle properties. The splitting of the  $P_i$  peak measures only the metabolic properties of the fiber, whereas the balance of ATP supply and demand embodied in the  $P_i$ /PCr

level can be achieved by various combinations of breakdown and resynthesis capacities. The independence of these properties is apparent in the lack of an inverse correlation between an individual's ATPase rate and the recovery time constant found in this study. Instead of the relation predicted from conventional fiber typing, the properties of fibers fall along a continuum (22). Thus a functional measure of metabolic capacity separate from contractile cost ( $\sim P$ /twitch) is necessary to assess the key elements of muscle energy balance on an individual basis.

In conclusion, separation of contractile ATP use from oxidative ATP synthesis reveals a nearly 2-fold variation in cost per twitch and recovery time constants. The functional differences in PCr breakdown rates among our subjects are correlated with a metabolite marker of fiber type,  $P_i$ /ATP. We conclude that the individual differences in ATP cost per twitch reflect the underlying myosin isoform contents and distribution of fiber types. Similarly, the variation in recovery time constants in proportion to the range of mitochondrial contents of human muscle suggests that this measure reflects the oxidative capacity of the muscle. Thus human muscle varies among individuals not only in metabolic characteristics associated with energy supply but also in the contractile properties that set the energy demand of exercise.

We thank Drs. Thomas Beck and M. Elaine Cress for their contributions to this study. Dr. Sharon Jubrias provided helpful comments on the text. Funding was provided by the Departments of Radiology and Rehabilitation Medicine of the University of Washington and from two grants from the National Institutes of Health AR38782 (M.J.K.) and AGAR 10853 (K.E.C.).

- Sweeney, H. L., Kushmerick, M. J., Mabuchi, K., Sreter, F. A. & Gergely, J. (1988) *J. Biol. Chem.* **263**, 9034–9039.
- Crow, M. T. & Kushmerick, M. J. (1982) *J. Gen. Physiol.* **79**, 147–166.
- Kushmerick, M. J., Meyer, R. A. & Brown, T. R. (1992) *Am. J. Physiol.* **263**, C598–C606.
- Dudley, G., Tullson, P. & Terjung, R. (1987) *J. Biol. Chem.* **262**, 9109–9114.
- Vandenborne, K., McCully, K., Kakihira, H., Prammer, M., Bolinger, L., Detre, J. A., De Meirleir, K., Walter, G., Chance, B. & Leigh, J. S. (1991) *Proc. Natl. Acad. Sci. USA* **88**, 5714–5718.
- Park, J. H., Brown, R. L., Park, C. R., McCully, K., Cohn, M., Haselgrove, J. & Chance, B. (1987) *Proc. Natl. Acad. Sci. USA* **84**, 8976–8980.
- Kent-Braun, J., McCully, K. & Chance, B. (1990) *J. Appl. Physiol.* **69**, 1165–1170.
- McCully, K., Boden, B., Tuchler, M., Fountain, M. & Chance, B. (1989) *J. Appl. Physiol.* **67**, 926–932.
- Blei, M. L., Conley, K. E. & Kushmerick, M. J. (1993) *J. Physiol. (London)* **465**, 203–222.
- Nelson, S. & Brown, T. R. (1989) *J. Magn. Res.* **84**, 95–109.
- Nelson, S. & Brown, T. R. (1987) *J. Magn. Res.* **75**, 229–243.
- Richards, T., Davis, C., Barker, B., Beinert, W. & Genant, H. (1987) *Invest. Radiol.* **22**, 741–746.
- Heineman, F. W., Eng, J., Berkowitz, B. A. & Balaban, R. S. (1990) *Magn. Reson. Med.* **13**, 490–497.
- Kushmerick, M. J., Moerland, T. R. & Wiseman, R. W. (1992) *Proc. Natl. Acad. Sci. USA* **89**, 7521–7525.
- Edström, L., Hultman, E., Sahlin, K. & Sjöholm, H. (1982) *J. Physiol. (London)* **332**, 47–58.
- Söderlund, K. & Hultman, E. (1991) *Am. J. Physiol.* **261**, E737–E741.
- Bárány, M. (1967) *J. Gen. Physiol.* **50**, 197–216.
- Chasiotis, D., Bergström, M. & Hultman, E. (1987) *J. Appl. Physiol.* **63**, 167–174.
- Meyer, R. (1988) *Am. J. Physiol.* **257**, C1149–C1157.
- Howald, H., Hoppeler, H., Claassen, H., Mathieu, O. & Straub, R. (1985) *Pflügers Arch.* **403**, 369–376.
- Achten, E., Cauteren, M. V., Willem, R., Luypaert, R., Malaisse, W. J., Bosch, G. V., Delanghe, G., Meirleir, K. D. & Osteaux, M. (1990) *J. Appl. Physiol.* **68**, 644–649.
- Pette, D. & Staron, R. (1990) *Rev. Physiol. Biochem. Pharmacol.* **116**, 1–76.

<sup>||</sup>Mizuno, M., Secher, N. & Quistorff, B., 21st Annual Meeting of the Society of Magnetic Resonance Medicine, Berlin, August 1992, Vol. 11, p. 779 (abstr.).